Bulletin of the Earthquake
Research Institute
Vol. 48 (1970), pp. 669-689

36. *Theoretical Seismograms and Earthquake Mechanism Part III. Azimuthal Variation of the Initial Phase of Surface Waves.*

By Toshikazu Odaka and Tatsuo Usami,
Earthquake Research Institute.

(Read on July 21, 1970.—Received on July 31, 1970.)

Abstract

Displacements of the spheroidal and torsional oscillations excited by a double couple point source of dip-slip type located in a radially heterogeneous earth are calculated at various stations on the free surface.

Calculations are performed using fundamental modes with colatitudinal order number $n=0\sim2000$, namely, those with period larger than about 6 seconds.

The azimuthal variation of the initial phase of surface waves is investigated by comparing the values obtained by Fourier analysis of synthetic seismograms with the ones defined theoretically by excitation functions of the free oscillation. Coincidence of the two patterns of the azimuthal variation of the initial phase is excellent. This suggests the possibility of estimating a source time function from the analysis of the phase angle of observed seismograms.

§ 3.1 Introduction

In the previous paper [Usami *et al.* (1970)], a method of calculating theoretical seismograms due to various force systems in a radially heterogeneous sphere was developed, and the effects of time functions on surface waves were considered. Calculations were limited to the displacements at a fixed point on the surface of the earth.

In this paper, calculations of the theoretical displacement at points equally distributed along the equator are carried out employing a certain time function. Radiation patterns of the amplitude and the phase of surface waves are given.

Radiation patterns for Rayleigh waves generated by dipolar point sources in a homogeneous isotropic half-space were calculated by Haskell [1963]. Radiation patterns for Rayleigh and Love waves from buried point sources in a flat stratified earth were examined by Ben-Menahem and Harkrider [1964] and formulated by Haskell [1964] as well.

Seismograms due to a normal dip-slip point source with 60° dip angle and 5.35 km depth are calculated. An epicenter is fixed at the north pole. Modes having periods larger than about 6 seconds are synthesized. A ramp function with rise time 45 seconds is assumed at the source. Since only the fundamental modes are considered in the numerical calculation, synthesized seismograms mainly refer to surface waves, that is, Rayleigh and Love waves.

The azimuthal variation of the spatial factor of the initial phase calculated from synthetic seismograms by means of Fourier analysis is in good agreement with that of the theoretical spatial phase which is determined from the excitation functions of the free oscillation.

The study suggests that the knowledge of the initial phase of surface waves of actual earthquakes will be useful for discriminating the source time function as well as for determining the phase velocity and the source mechanism.

§ 3.2 Calculation of the Spatial Factor of the Initial Phase

The initial phase of surface waves has been used by several seismologists for the study of focal mechanisms and source functions [Aki (1960), Brune (1961), Ben-Menahem and Toksöz (1963)]. The phase velocity of surface waves can be determined from seismograms at two stations on the same great circle path by means of Fourier transform [Satô (1955, 1956, 1958)]. It is given by the formula [*e.g.* Toksöz and Anderson (1966)]

$$C(p)=\frac{\Delta_2-\Delta_1}{(t_2-t_1)+(1/p)[\phi_2(p)-\phi_1(p)+2\pi N]}, \qquad (3\cdot2\cdot1)$$

where $\Delta_2-\Delta_1$ is the distance between the two stations, t_1 and t_2 the initial times of Fourier windows, $\phi_1(p)$ and $\phi_2(p)$ the phase delays relative to the beginning of the windows, N an integer and p the angular frequency.

If we know the phase at $\Delta_1=t_1=0$, the phase velocity can be calculated from data at a single station by the formula

$$C(p)=\frac{\Delta}{t+(1/p)[\phi(p)-\phi_{int}(p)+2\pi N]}, \qquad (3\cdot2\cdot2)$$

where Δ denotes the epicentral distance, t the initial time of the Fourier window, $\phi(p)$ the phase delay relative to the beginning of the window and $\phi_{int}(p)$ the initial phase.

From the relation (3·2·2), we have

$$\phi_{int}(p)=p\cdot(t-\Delta/C(p))+\phi(p)+2\pi N \qquad (3\cdot2\cdot3)$$

The initial phase is easily determined from this relation, if the phase velocity is known. This definition of the initial phase is opposite in sign to that of Brune *et al.* [1960] and Brune [1961]. This comes from that the phase angle is defined as $\exp(-j\cdot\phi(p))$ in the present paper, where j means the unit of imaginary numbers.

The source characteristic is assumed to be specified as a product of three factors [Ben-Menahem and Toksöz (1963)], namely, the spatial, temporal and propagation factors. Since a point source is assumed, the propagation factor does not appear in the present study.

Describing the Fourier transform of a source time function as

$$f^*(p)=|f^*(p)|\,e^{-j\,\phi_{tm}(p)}\,, \tag{3·2·4}$$

the spatial factor of the initial phase will be given as

$$\phi_{sp}(p)=\phi_{int}(p)-\phi_{tm}(p)\,. \tag{3·2·5}$$

From the formulas (3·2·3) and (3·2·5), we have

$$\phi_{sp}(p)=p\cdot(t-\Delta/C(p))+\phi(p)-\phi_{tm}(p)+2\pi N\,. \tag{3·2·6}$$

This relation makes possible to calculate the spatial factor of the initial phase under the assumption that the value of the phase velocity and the temporal phase factor ϕ_{tm} are known. On the other hand, the phase of a source time function, namely, the temporal phase factor will be estimated, if the spatial phase and the phase velocity are given. The latter case is more important in the analysis of actual seismograms, since the spatial phase can be estimated theoretically under suitable assumptions as will be seen in later section. Here, care must be taken for that the spatial phase defined by expression (3·2·6) involves the phases due to the polar phase shift and the phase advance in leaving source.

As to much simpler sources, such as localized stresses applied around the pole, the calculations of the initial phase from theoretical seismograms were carried out in the previous papers [Satô *et al.* (1963), Usami *et al.* (1968)].

§ 3.3 Theoretical Seismogram and Radiation Pattern

Figures 1, 2 and 3 show displacements on the surface of the earth due to a normal dip-slip point source with 60° dip angle and 5.35 km depth. The direction of the fault is taken as the direction $\varphi=0°$. The source time function is assumed to be a ramp function whose rise time is about 45 seconds. Its Fourier transform is given by

$$(1/p)\{\sin(pt_0/2)/(pt_0/2)\}\exp[-j(pt_0/2+\pi/2)]\,,$$

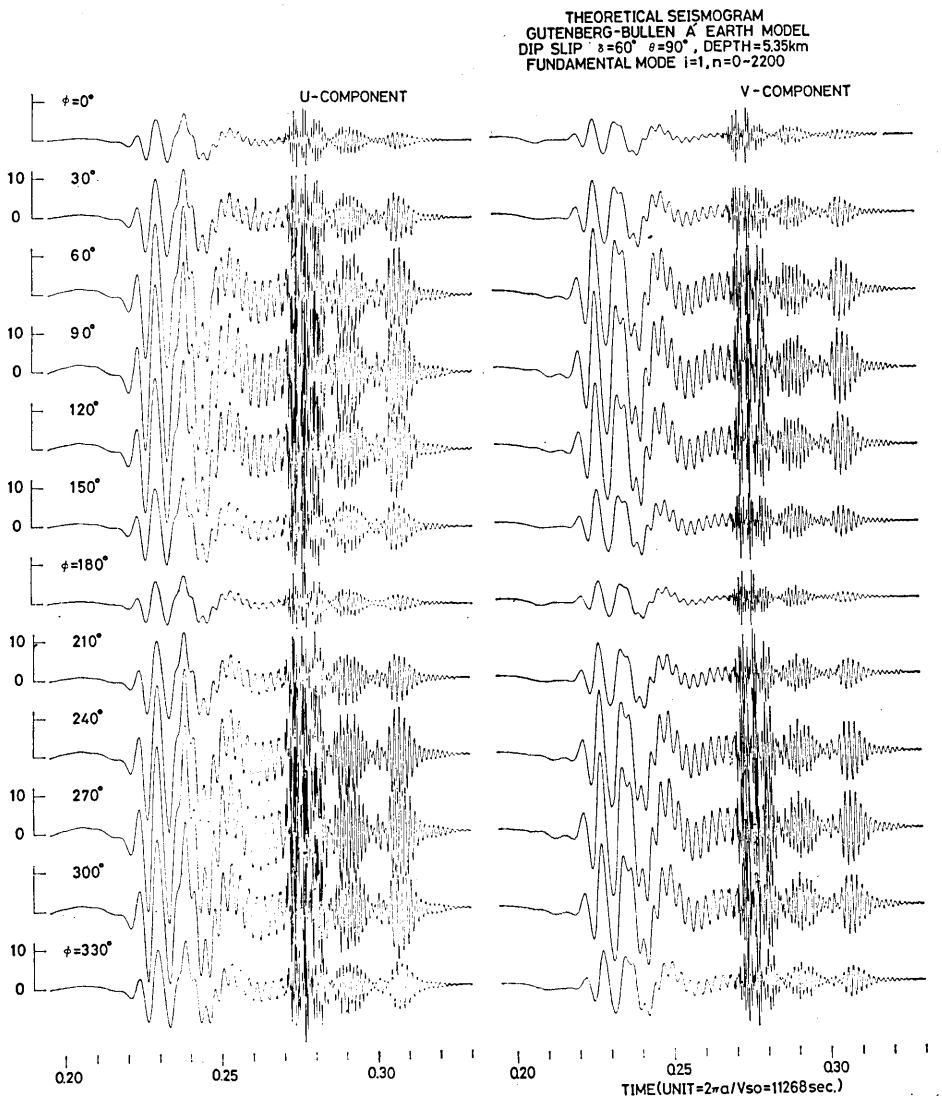

Fig. 1. Vertical disturbances, which correspond to Rayleigh waves.

Fig. 2. Colatitudinal component, which involves both Rayleigh and Love waves.

Fig. 1~3. Theoretical seismograms of displacements excited by a normal dip-slip point source with 60° dip angle at 5.35 km depth in a Gutenberg-Bullen A′ spherical earth. A ramp function with a rise time of 45 sec. is assumed as the source time function. The unit of time is taken

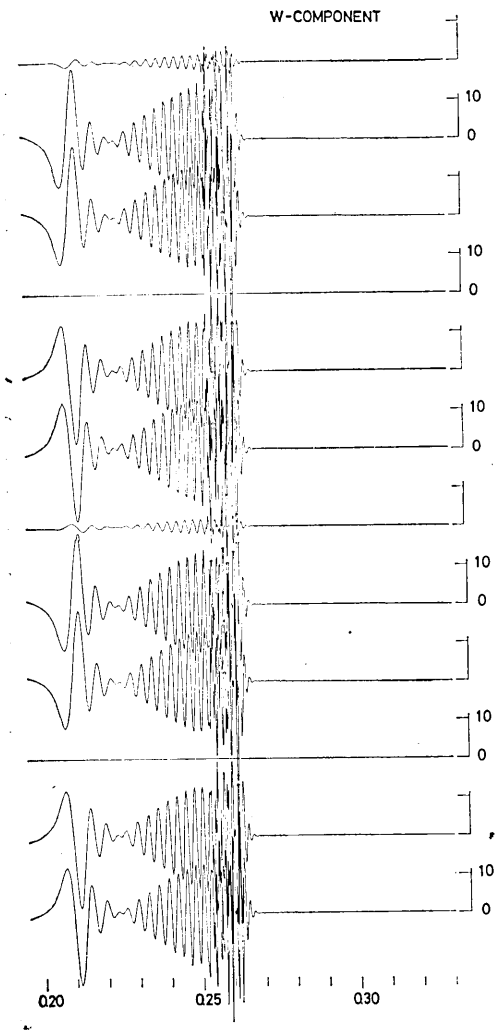

Fig. 3. Azimuthal component, which involves both the spheroidal and torsional oscillations. Since the spheroidal component is negligibly small compared with the torsional one, the seismogram expresses Love waves.

as $2\pi a/v_{SO}=11268$ sec. The ordinate scale is the same as on Fig. 14 in the previous paper [Usami *et al.* (1970)].

where p denotes the angular frequency and t_0 the rise time. The temporal phase factor is, therefore, easily assigned as $(pt_0/2+\pi/2)$ in the present case. A Gutenberg-Bullen A′ earth model [Usami *et al.* (1966)] is assumed.

The theoretical seismograms were calculated at 17 points on the equator with azimuths $\varphi=0°$ (30°) 330°, 15°, 45°, 165°, 195° and 345° for the time interval $t=0.195$ (0.00025) 0.33 which covers the passage of Rayleigh and Love waves. The unit of time is $2\pi a/v_{SO}$, namely, 11268 seconds, where a is the radius of the earth and v_{SO} the shear wave velocity on the surface.

Synthetic seismograms represent surface waves, since only the fundamental modes having colatitudinal order numbers from 0 to about 2000, covering periods larger than about 6 seconds, are superposed in the present study.

The radial component (u) consists of the spheroidal oscillation alone, and colatitudinal (v) and azimuthal (w) components involve both spheroidal and torsional oscillations. The spheroidal component of the azimuthal displacement, however, is negligibly small compared with the torsional. The u component is considered to represent the vertical displacement of Rayleigh wave, and the w component the azimuthal displacement of Love wave.

As apparent from Figures

1, 2 and 3, the radiation patterns of the amplitude of the radial and colatitudinal components are expected to show two sectors over the whole frequency range, and that of the azimuthal component to show a typical four-lobed pattern.

As for the azimuthal variation of the phase angle, the azimuthal components may indicate a four-lobed pattern as the amplitude factor does, because each wave train changes its sign in crossing a quadrant border. The phase factors of the radial and colatitudinal components, however, do not necessarily show two-lobed patterns, which is different from those of amplitude. For instance, wave trains with long periods do not suffer any phase change over the whole azimuthal angle.

These expectations are ascertained by calculating the spatial factor of the initial phase from these seismograms using the expression (3·2·6) and the value of phase velocity given in the previous report [Usami *et al.* (1970)].

These results are shown in Figures 4, 5, 6 and 7 in which open and solid circles and squares indicate thus obtained values. These values will be called the "observed spatial phase". This procedure is useful for obtaining the spatial phase from actual seismograms.

§ 3.4 Theoretical Spatial Phase

The spatial factor of the initial phase which appeared in the preceding section is to be inherent in the source geometry and the response of the medium except for constant values. This indicates that the spatial phase of surface waves should be expressed as a function of parameters expressing the source geometry and the earth model. Expressions of the spatial phase by the excitation functions of the free oscillation are given in the following.

A detailed study of the calculation of the free oscillation excited by a single force, couple and double couple point sources is given in the previous paper [Usami *et al.* (1970)]. The expressions of displacement are summarized here in a more compact way.

Radial, colatitudinal and azimuthal components of displacement of the spheroidal oscillation due to a double couple point source are

$$\left.\begin{aligned}
u(r,\theta,\varphi,t) &= -j\cdot C\sum_n f^*(p_n)\, e^{jp_n t} U_n(r) \\
&\quad\times[d_0\cdot S_n^{(0)} P_n(\cos\theta) + d_1\cdot S_n^{(1)} P_n^{\,1}(\cos\theta) + d_2\cdot S_n^{(2)} P_n^{\,2}(\cos\theta)] \\
v(r,\theta,\varphi,t) &= -j\cdot C\sum_n f^*(p_n)\, e^{jp_n t}\, V_n(r) \\
&\quad\times[d_0\cdot S_n^{(0)} \dot{P}_n(\cos\theta) + d_1\cdot S_n^{(1)} \dot{P}_n^{\,1}(\cos\theta) + d_2\cdot S_n^{(2)} \dot{P}_n^{\,2}(\cos\theta)] \\
w(r,\theta,\varphi,t) &= -j\cdot C\sum_n f^*(p_n)\, e^{jp_n t}\, V_n(r)
\end{aligned}\right\} \quad (3\cdot4\cdot1)$$

$$\times\left[d_3\cdot S_n^{(1)}\frac{P_n^{\,1}(\cos\theta)}{\sin\theta}+d_4\cdot S_n^{(2)}\frac{2P_n^{\,2}(\cos\theta)}{\sin\theta}\right]$$

where, for the case of dip-slip

$$d_0=\frac{\sin 2\delta}{2},\quad d_1=\cos 2\delta\cdot\sin\varphi,\quad d_2=\frac{\sin 2\delta}{2}\cdot\cos 2\varphi,\quad d_3=\cos 2\delta\cdot\cos\varphi,$$
$$d_4=-\frac{\sin 2\delta}{2}\cdot\sin 2\varphi,$$

and for the case of strike-slip

$$d_0=0,\quad d_1=\cos\delta\cdot\cos\varphi,\quad d_2=-\sin\delta\cdot\sin 2\varphi,\quad d_3=-\cos\delta\cdot\sin\varphi,$$
$$d_4=-\sin\delta\cdot\cos 2\varphi.$$

Displacements of the torsional oscillation are

$$\left.\begin{aligned}
&u(r,\theta,\varphi,t)=0,\\
&v(r,\theta,\varphi,t)=-j\cdot C\sum_n f^*(p_n)\,e^{jp_nt}\,W_n(r)\\
&\qquad\times\left[h_1\cdot T_n^{(1)}\frac{P_n^{\,1}(\cos\theta)}{\sin\theta}+h_2\cdot T_n^{(2)}\frac{2P_n^{\,2}(\cos\theta)}{\sin\theta}\right]\\
&w(r,\theta,\varphi,t)=-j\cdot C\sum_n f^*(p_n)\,e^{jp_nt}\,W_n(r)\\
&\qquad\times[-h_3\cdot T_n^{(1)}\dot{P}_n^{\,1}(\cos\theta)-h_4\cdot T_n^{(2)}\dot{P}_n^{\,2}(\cos\theta)]
\end{aligned}\right\}\quad(3\cdot4\cdot2)$$

where, for the dip-slip case

$$h_1=\cos 2\delta\cdot\sin\varphi,\quad h_2=\frac{\sin 2\delta}{2}\cdot\cos 2\varphi,\quad h_3=-\cos 2\delta\cdot\cos\varphi,\quad h_4=\frac{\sin 2\delta}{2}\cdot\sin 2\varphi,$$

and for the strike-slip case

$$h_1=\cos\delta\cdot\cos\varphi,\quad h_2=-\sin\delta\cdot\sin 2\varphi,\quad h_3=\cos\delta\cdot\sin\varphi,\quad h_4=\sin\delta\cdot\cos 2\varphi.$$

r,θ and φ represent the polar coordinates referred to the earth's center. δ gives the dip angle and dot $(\cdot)$ on the associated Legendre function $P_n^{\,m}(\cos\theta)$ denotes $d/d\theta$ and p_n the eigen-frequency in radians.

The other coefficients are

$$\left.\begin{aligned}
&C=\frac{M_0}{4\pi a^3}\,\frac{v_{so}}{b},\\
&S_n^{(0)}=(2n+1)\left[-\frac{2(3\lambda+2\mu)}{\lambda+2\mu}U_n(b)\right.\\
&\qquad\left.+\frac{3\lambda+2\mu}{\lambda+2\mu}n(n+1)\,V_n(b)+\frac{2b}{\lambda+2\mu}E_S(b)\right]\Big/\frac{\partial E_S(a)}{\partial\eta},
\end{aligned}\right.$$

$$\left.\begin{aligned} S_n^{(1)} &= (2n+1)\frac{b}{\mu}E_T(b)\Big/\frac{\partial E_S(a)}{\partial \eta}, \quad S_n^{(2)} = (2n+1)\,V_n(b)\Big/\frac{\partial E_S(a)}{\partial \eta} \\ T_n^{(1)} &= (2n+1)\frac{b}{n(n+1)\mu}E_{TT}(b)\Big/\frac{\partial E_{TT}(a)}{\partial \eta}, \\ T_n^{(2)} &= (2n+1)\frac{1}{n(n+1)}W_n(b)\Big/\frac{\partial E_{TT}(a)}{\partial \eta}, \end{aligned}\right\} \quad (3\cdot4\cdot3)$$

where M_0 means the seismic moment, a the radius of the earth, b the radius of the source surface, v_{S0} the shear wave velocity at the earth surface, λ and μ the Lame's constants at the source depth, η the non-dimensional frequency of the free oscillation, $U_n(r)$, $V_n(r)$ and $W_n(r)$ the functions giving the radial distribution of u, v and w and E_S, E_T and E_{TT} the radial, colatitudinal and azimuthal components of stress.

$S_n^{(0)}$, $S_n^{(1)}$, $S_n^{(2)}$, $T_n^{(1)}$ and $T_n^{(2)}$ are the medium response functions which depend on the earth model and the source depth. The excitation function is defined as the product of these functions and the factors related to the dip angle in the coefficients d_i and h_i.

Asymptotic formulas of the associated Legendre functions, which hold for order numbers corresponding to the period range of ordinary surface waves, are useful for the phase study of each mode of the free oscillation.

These are

$$\left.\begin{aligned} P_n^m(\cos\theta) &\sim (-1)^m n^m \sqrt{\frac{2}{n\pi \sin\theta}} \cdot \cos[(n+1/2)\theta + m\pi/2 - \pi/4], \\ \dot{P}_n^m(\cos\theta) &\sim (-1)^m n^{m+1} \sqrt{\frac{2}{n\pi \sin\theta}} \cdot \cos[(n+1/2)\theta + m\pi/2 + \pi/4]. \end{aligned}\right\} \quad (3\cdot4\cdot4)$$

$$(0<\theta<\pi)$$

Hence, we have

$$\left.\begin{aligned} P_n(\cos\theta) &\sim k_n \cdot \cos[(n+1/2)\theta - \pi/4], \\ P_n^1(\cos\theta) &\sim nk_n \cdot \sin[(n+1/2)\theta - \pi/4], \\ P_n^2(\cos\theta) &\sim -n^2 k_n \cdot \cos[(n+1/2)\theta - \pi/4], \\ \dot{P}_n(\cos\theta) &\sim nk_n \cdot \cos[(n+1/2)\theta + \pi/4], \\ \dot{P}_n^1(\cos\theta) &\sim n^2 k_n \cdot \sin[(n+1/2)\theta + \pi/4], \\ \dot{P}_n^2(\cos\theta) &\sim -n^3 k_n \cdot \cos[(n+1/2)\theta + \pi/4], \end{aligned}\right\} \quad (3\cdot4\cdot5)$$

where,

$$k_n = \sqrt{\frac{2}{n\pi \sin\theta}}.$$

Using these formulas, the expressions (3·4·1) at the earth surface can be reduced to

$$\left.\begin{aligned} u(a,\theta,\varphi,t) &= -j\cdot C\sum_n f^*(p_n)\,e^{jp_nt}\,U_n(a)\cdot k_n\{(S_n^{(0)}\cdot d_0-n^2S_n^{(2)}\cdot d_2)\\ &\quad\times\cos[(n+1/2)\theta-\pi/4]+nS_n^{(1)}\cdot d_1\sin[(n+1/2)\theta-\pi/4]\},\\ &= C\sum_n |f^*(p_n)|\,U_n(a)\,k_n\cdot S_n^{(u)}\,e^{j[p_nt-\phi_{tm}-\pi/2]}\\ &\quad\times\cos[(n+1/2)\theta-\pi/4-\alpha_n^{(u)}], \end{aligned}\right\} \quad (3\cdot4\cdot6)$$

$$\begin{aligned} &= \frac{C}{2}\sum_n |f^*(p_n)|\,U_n(a)\,k_n\cdot S_n^{(u)}\{e^{j[p_nt-(n+1/2)\theta-\pi/4+\alpha_n{}^{(u)}-\phi_{tm}]}\\ &\quad+e^{j[p_nt+(n+1/2)\theta-3\pi/4-\alpha_n{}^{(u)}-\phi_{tm}]}\}, \end{aligned} \quad (3\cdot4\cdot7)$$

where

$$\left.\begin{aligned} f^*(p) &= |f^*(p)|\,e^{-j\phi_{tm}(p)},\\ S_n^{(u)} &= [(S_n^{(0)}\cdot d_0-n^2S_n^{(2)}\cdot d_2)^2+(nS_n^{(1)}\cdot d_1)^2]^{1/2},\\ \alpha_n^{(u)} &= \tan^{-1}\frac{nS_n^{(1)}\cdot d_1}{S_n^{(0)}\cdot d_0-n^2S_n^{(2)}\cdot d_2}. \end{aligned}\right\} \quad (3\cdot4\cdot8)$$

Similar expressions are obtained for the colatitudinal and azimuthal displacements of the spheroidal oscillation. For the torsional oscillation, equations (3·4·2) can be transformed similarly. Actual numerical calculation is, of course, done taking the real part of these expressions.

The expression (3·4·7) means that each mode of the free oscillation, which is represented as a standing wave in (3·4·6), is expressed as a sum of waves traveling in mutually opposite directions.

From formulas (3·2·5) and (3·4·7) and considering that the value of $U_n(a)$ is identically taken as unity, the spatial factor of the initial phase of waves propagating on a spherical earth in the $+\theta$ direction is obtained as

$$\phi_{sp}(p)=\pi/4-\alpha_n^{(u)}, \quad (3\cdot4\cdot9)$$

and that of waves propagating in the $-\theta$ direction as

$$\phi_{sp}(p)=-\pi/4+\alpha_n^{(u)}. \quad (3\cdot4\cdot10)$$

In deriving the formula (3·4·10) from (3·4·7), the epicentral distance of the station for the wave propagating along the major arc of a great circle path was taken as $2\pi-\theta$. The spatial phase of every component of the spheroidal and torsional oscillations is summarized in Table 1, which will be called the "theoretical spatial phase". Special attention must be given to the fact that these "theoretical spatial phases" are functions of the earth model, dip angle of a fault plane, the focal depth and the azimuth of the station.

Table 1. The theoretical spatial factors of the initial phase of surface waves generated by a double couple point source in a radially heterogeneous sphere. u_n, v_n and w_n are the radial, colatitudinal and azimuthal components of displacement having the order number n. d_i, h_i, S_n and T_n are quantities defined in the equations (3·4·1), (3·4·2) and (3·4·3).

		Waves propagating in $+\theta$ direction	Waves propagating in $-\theta$ direction
Spheroid	u_n	$\pi/4-\alpha_n^{(u)}$	$-\pi/4+\alpha_n^{(u)}$
	v_n	$-\pi/4-\alpha_n^{(u)}$	$\pi/4+\alpha_n^{(u)}$
	w_n	$-3\pi/4-\alpha_n^{(w)}$	$3\pi/4+\alpha_n^{(w)}$
Torsion	v_n	$-3\pi/4-\beta_n^{(v)}$	$3\pi/4+\beta_n^{(v)}$
	w_n	$3\pi/4+\beta_n^{(w)}$	$-3\pi/4-\beta_n^{(w)}$

$$\alpha_n^{(u)}=\tan^{-1}\left[\frac{nd_1S_n^{(1)}}{d_0S_n^{(0)}-n^2d_2S_n^{(2)}}\right],\qquad \alpha_n^{(w)}=\tan^{-1}\left[\frac{nd_3S_n^{(1)}}{2n^2d_4S_n^{(2)}}\right]$$

$$\beta_n^{(v)}=\tan^{-1}\left[\frac{nh_1T_n^{(1)}}{2n^2h_2T_n^{(2)}}\right],\qquad \beta_n^{(w)}=\tan^{-1}\left[\frac{nh_3T_n^{(1)}}{n^2h_4T_n^{(2)}}\right]$$

The expressions are very similar to those for a flat layered model obtained by Ben-Menahem and Toksöz [1963], although the medium response functions are different from each other.

A constant phase difference $\pi/2$ or $-\pi/2$ between waves radiated in opposite directions means the polar phase shift [Brune *et al.* (1961)]. Strictly speaking of the initial phase, a correction must be applied for waves passing the pole or antipode to remove these effects. Constant terms of the spatial phases of waves traveling in the $+\theta$ direction show the phase advance in leaving the source. If we disregard these constants, the spatial phase of a wave propagating in the $-\theta$ direction is opposite in sign and is equal in its absolute value to that traveling in the $+\theta$ direction. That will, also, be apparent if the effect of the azimuthal angle on the theoretical spatial phase is considered (see $\alpha_n^{(u)}$ of the equation (3·4·8)). This conclusion is important, because when we calculate the phase velocity from combination of waves such as R_1-R_3, R_2-R_4, these phase factors cancel each other, but for combinations such as R_1-R_2, R_2-R_3, their effect remains except for special cases having particular azimuthal angles or source geometry. This will also be true in calculating the differential phase [Ben-Menahem (1961)] of two opposite-going waves from a finite moving source. Similar conclusions hold for Love waves. Here, attention must be paid to the fact that the "theoretical spatial phase" is attached to each component wave with an eigenfrequency.

§ 3.5 Comparison between the Theoretical and Observed Spatial Phases

Comparison of the "observed spatial phase" with the "theoretical one" is done as is shown in Figures 4, 5, 6 and 7. Solid circles of Figures 4 and 5 denote the "observed one" and solid lines the "theoretical one". Coincidence of the observed and theoretical spatial phases is excellent. Broken lines give radiation patterns of the Fourier amplitude spectrum of the seismograms.

The amplitude of the radial component shows two-lobed patterns and that of the azimuthal component has four sectors. The azimuthal variation of the spatial phase is much more complicated. That of the vertical component of long period Rayleigh waves is nearly constant independent of the azimuthal angle and the pattern approaches the one corresponding to the two-lobed pattern of amplitude as the period of waves diminishes. The spatial phase of the azimuthal component of Love wave has four sectors though it is disturbed near the axis of the strike direction of the fault. Of course, these features are, to some extent, due to the source geometry and the earth model adopted in the present paper.

Since Rayleigh and Love waves are mingled in the colatitudinal component, seismograms synthesized separately for the spheroidal and torsional oscillations are used for calculation of the spatial phase. The results are shown by solid and open circles in Figure 6. Solid and broken lines are the "theoretical spatial phases". The source geometry is the same as in the previous case.

So far, waves propagating along the minor arc of a great circle path are considered. We next consider the case of R_2 wave which propagates along the major arc. At first, the theoretical disturbance of the R_2 wave was computed, using a group-velocity window. The spatial phases calculated from these seismograms are denoted by circles and squares in Figure 7. Solid and broken lines are the "theoretical ones". As mentioned previously, the spatial phases of our figures are not corrected for the polar phase shift and the phase advance in leaving the source. These terms, however, are not important for examining the azimuthal variation of the initial phase, since they are constant independent of the frequency and azimuthal angle.

It is noteworthy that both spatial phases, one calculated from the theoretical seismogram which is synthesized by superposition of a large number of modes of the free oscillation and the other from the excitation function which holds for each mode of vibration, coincide well (refer to Appendix (a)). This indicates that the theoretical spatial phase may

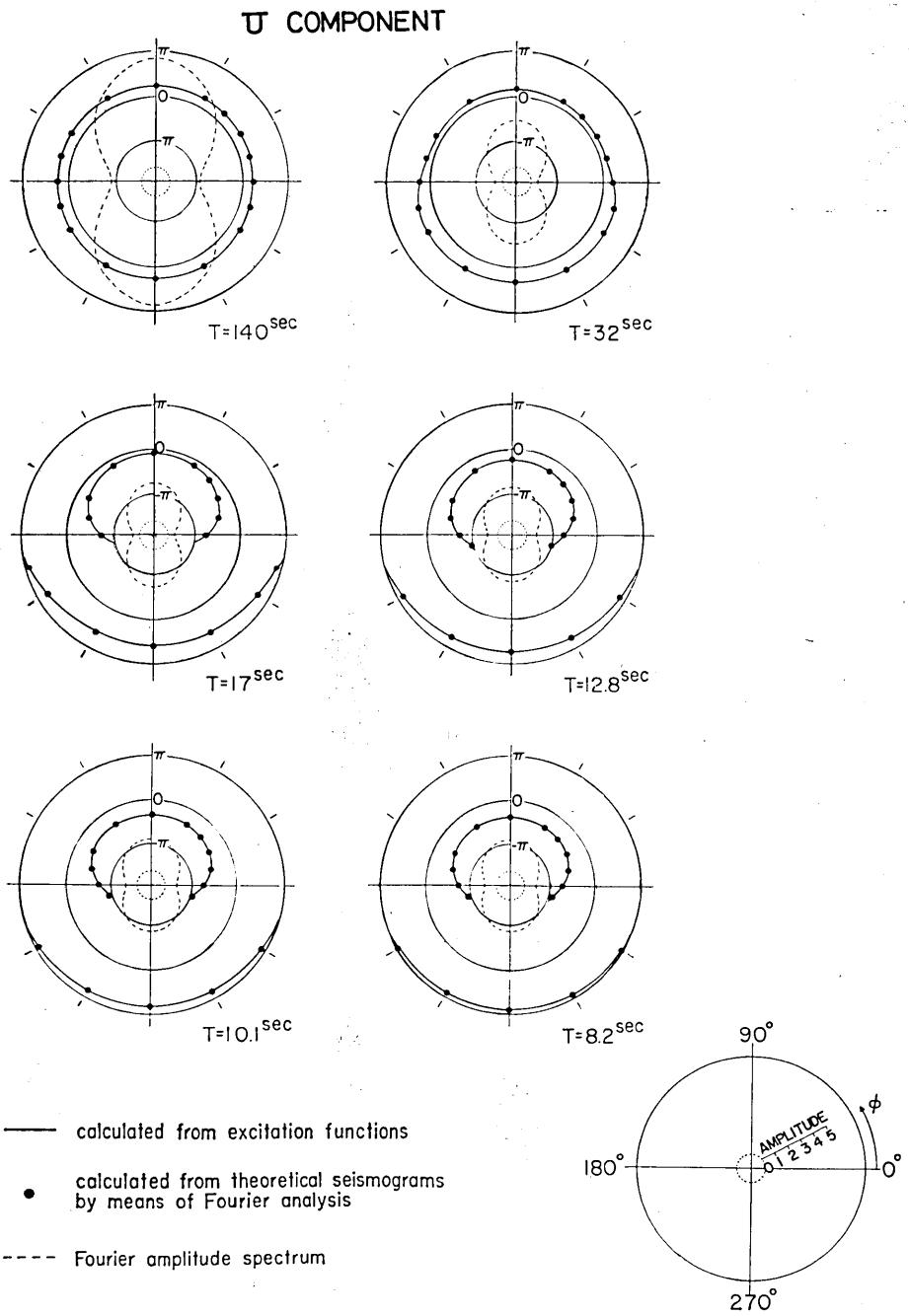

Fig. 4. Radiation patterns of amplitude and spatial phase of the vertical displacement of Rayleigh waves generated by a normal dip-slip point source in the Gutenberg-Bullen A′ spherical earth. The dip angle is 60° and the focal depth 5.35 km. T denotes the period. The scale of the Fourier amplitude is taken arbitrarily, but is consistent in Figures 4 and 5.

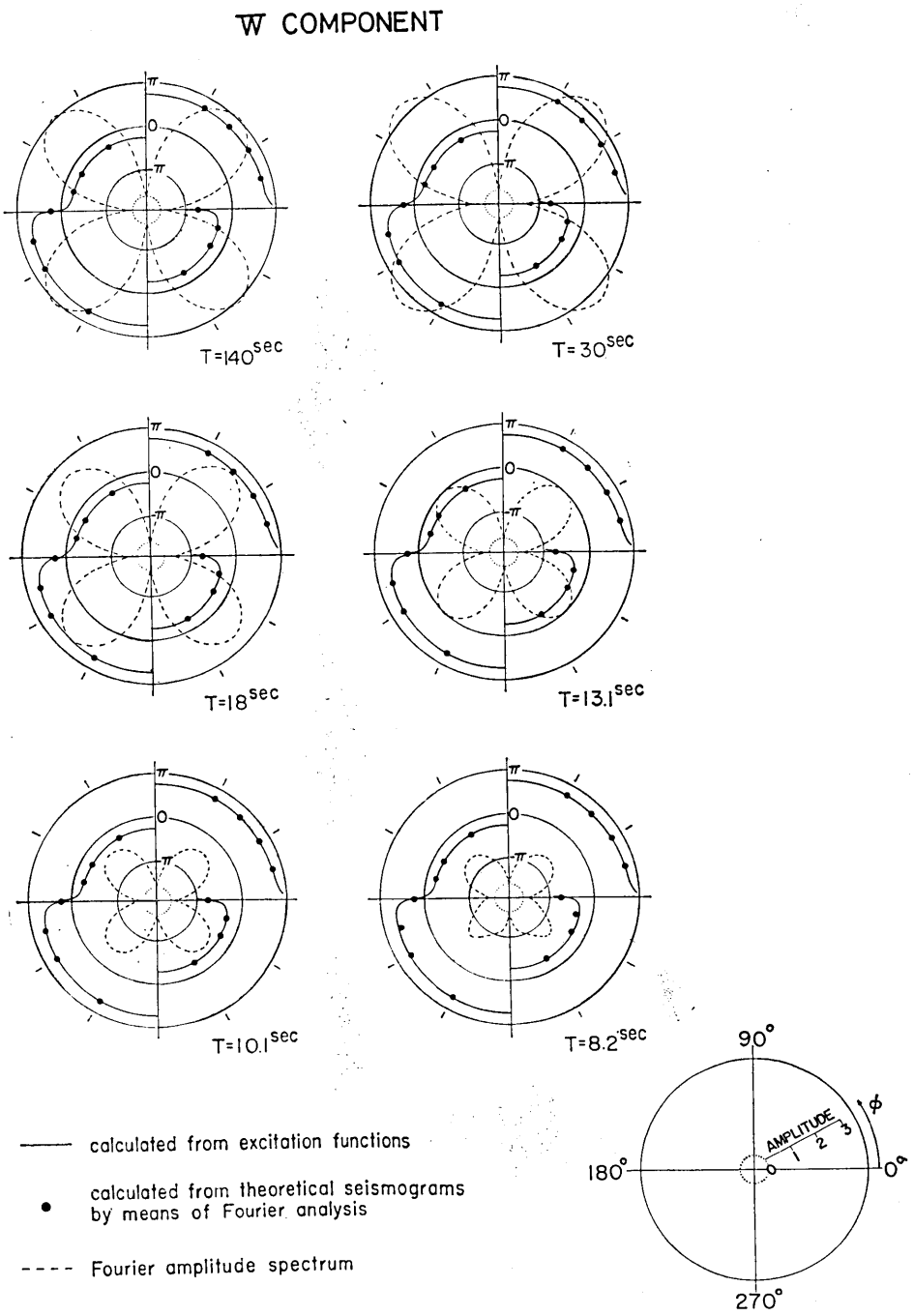

Fig. 5. Radiation patterns of amplitude and spatial phase of the azimuthal component of Love waves. The earth model and the source geometry are the same as in Figure 4.

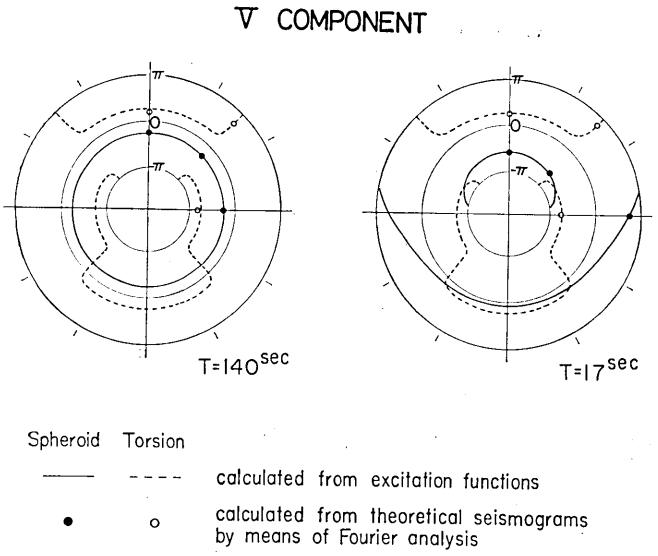

Fig. 6. The azimuthal variation of the spatial factor of the initial phase of the co-latitudinal displacement of Rayleigh and Love waves. The earth model and the source geometry are the same as in Figure 4.

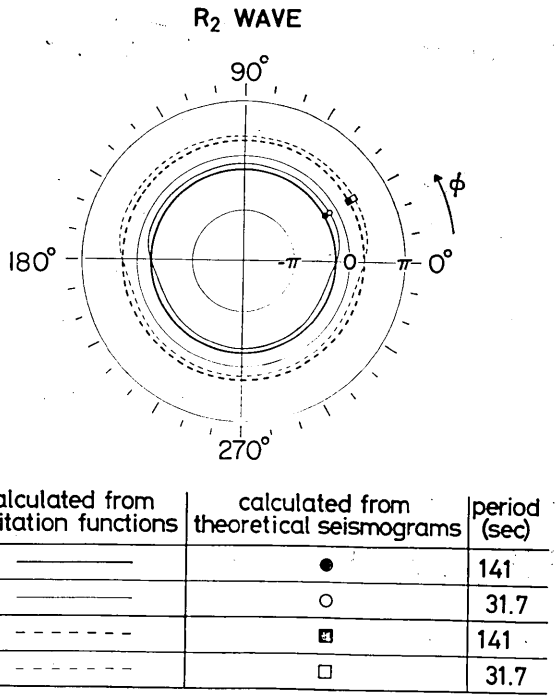

	calculated from excitation functions	calculated from theoretical seismograms	period (sec)
U	———	●	141
	———	○	31.7
V	- - - - - - -	■	141
	- - - - - - -	□	31.7

Fig. 7. Azimuthal variation of the spatial phase of vertical and horizontal components of R_2 wave. The earth model and the source geometry are the same as in Figure 4.

be useful for estimating the phase factor of a source time function ϕ_{tm} from observed seismograms, if the phase velocity data, source geometry and epicentral distance are known and an earth model is assigned. The procedure is, as was explained in section 3.2, similar to that used in the calculation of the spatial phase.

§ 3.6 Effects of Focal Depth on the Spatial Phase

In the preceding sections, the source is assumed to be located at 5.35 km depth. In this section, the effect of focal depth on the azimuthal variation of the spatial phase is investigated. Source parameters other than the focal depth are the same as before.

Surface displacements due to dip-slip point sources at various depths are computed at a point $\theta=90°$, $\varphi=0°$ on the surface, and shown in Figures 8, 9 and 10. From these figures, it will be noticed that the phase as well as the amplitude of surface waves is much affected by the focal depth.

In radial and colatitudinal components, the amplitude of a wave train of long period becomes very small at a certain source depth and increases again to some depth. In crossing the critical focal depth which corresponds to the smallest amplitude, the phase angle seems to shift by π. In the azimuthal component, on the other hand, the wave train of any periods seems not to suffer any phase change. For waves of shorter periods, it may be expected that the phase change occurs at shallower focal depths than 5.35 km.

The "theoretical spatial phase" was calculated from the excitation functions due to a source at each focal depth to see the effect of the focal depth on the azimuthal variation of the spatial phase. Soid lines in Figures 11, 12, 13 and 14 represent the results for some periods. Some features of the phase angle seen in theoretical disturbances are explained from these figures and Figures 4 and 5.

In the radial displacement, for example, the phase angle of a wave train with period about 150 sec. changes by π between the focal depths 51 and 112 km, and that of about 30 sec. does so between 5.35 and 26.7 km.

§ 3.7 Appendix

(*a*) *Standing wave and progressive wave*

The appendant result confirmed through numerical computations seems to be interesting from a viewpoint of the physical interpretation of wave propagation.

The vertical displacement of R_1 wave was computed at a point

($\theta=90°$, $\varphi=0°$) using the first term of equation (3·4·7), namely, the expression of waves propagating in the $+\theta$ direction. Modes with colatitudinal order number n larger than 40 were employed. The source geometry and the source time function are the same as those in section 3.3. It is found that thus calculated R_1 wave agree satisfactorily with that obtained by the equation (3·4·6) which shows the sum of standing waves and that the superposition of waves propagating in the $-\theta$ direction reveals displacements within the limits of the computational error. Thus, it is expected that the R_2 wave can be synthesized from the second term of the equation (3·4·7). The expectation was confirmed numerically. This fact indicates that, if wave trains traveling in opposite

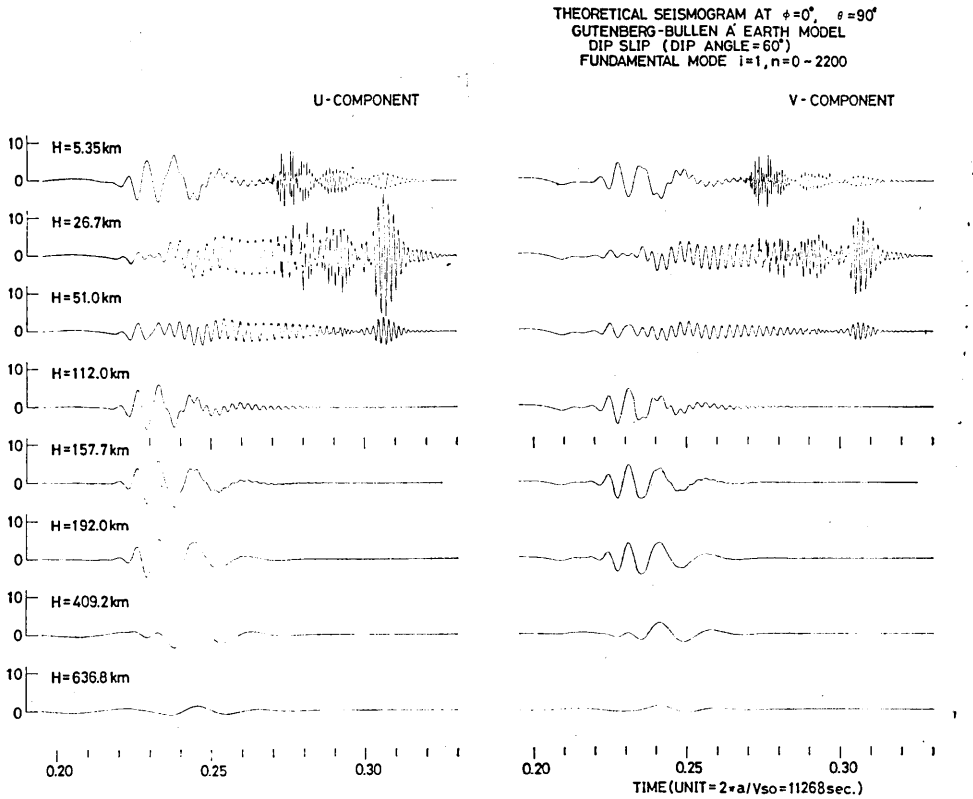

Fig. 8. Radial component, involving only the spheroidal oscillation.

Fig. 9. Colatitudinal displacement.

Fig. 8~10. Theoretical seismogram of disturbances excited by a normal dip-slip point source with 60° dip angle located at various focal depths in the Gutenberg-Bullen A′ spherical earth. A ramp function with a rise time of about 45 sec. is assumed at the source. The station is at $\theta=90°$, $\varphi=0°$ on the surface of the

directions appear separately in time, they are computed with sufficient accuracy from either the first or the second term of equation (3·4·7). In other words, the second or the first term of (3·4·7) is dummy in expressing waves propagating in a certain direction. This means that, although contribution of each mode of the dummy term has the same amplitude as the other term, the summation of modes belonging to dummy terms becomes negligible.

Therefore, both Rayleigh and Love waves used in the calculation in the previous sections will be expressed by either of the two opposite-going waves. This, in turn, guarantees the good agreement between the "theoretical spatial phase" and the "observed one", if we remember that the formula (3·2·3) or (3·2·6) is just the one to reduce the phase angle represented in the formula (3·4·7) to the one at the epicenter. Synthetic seismograms thus calculated do not, of course, include component waves with extremely long periods for which an asymptotic expansion of the associated Legendre function cannot hold.

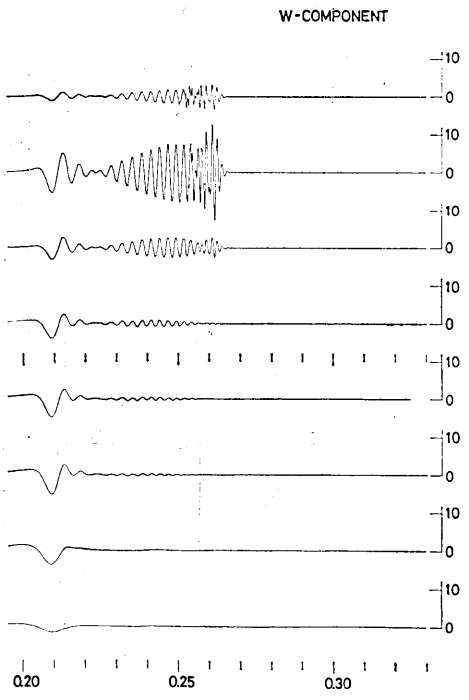

Fig. 10. Azimuthal displacement. Love wave is predominant, since the spheroidal component is negligibly small compared with the torsional.

earth. H indicates the focal depth. The scale of the ordinate and the abscissa is the same as in Figures 1~3.

(*b*) *Symmetrical Relations*

In the present paper, the spatial phase as well as the theoretical seismogram is calculated at azimuthal angles from 0° to 360°. In practice, however, calculations need not be carried out over this whole range, because there exist the following relations between the displacement components for different azimuths (see (3·4·1) and (3·4·2)):

for the dip-slip case

$$u(r, \theta, \varphi, t) = u(r, \theta, \pi-\varphi, t),$$
$$v(r, \theta, \varphi, t) = v(r, \theta, \pi-\varphi, t),$$
$$w(r, \theta, \varphi, t) = -w(r, \theta, \pi-\varphi, t), \qquad (3\cdot7\cdot1)$$

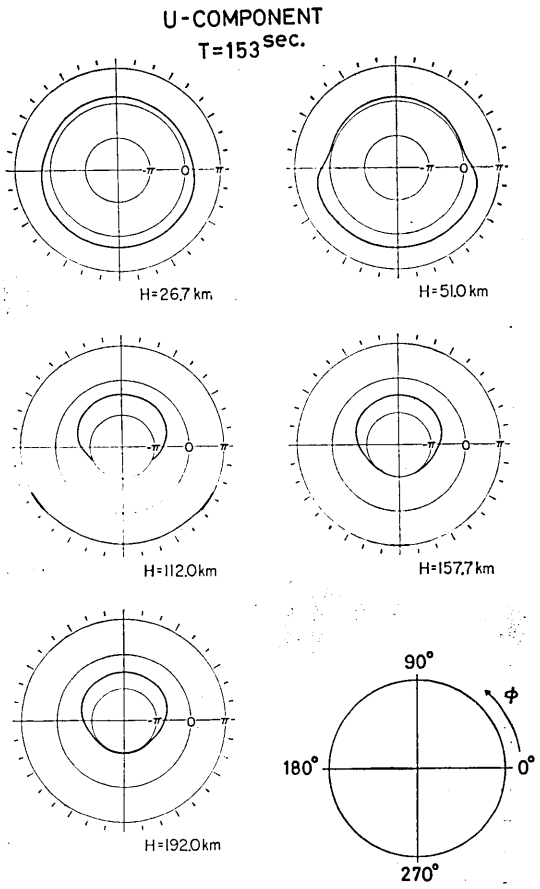

Fig. 11. Vertical component of Rayleigh wave.

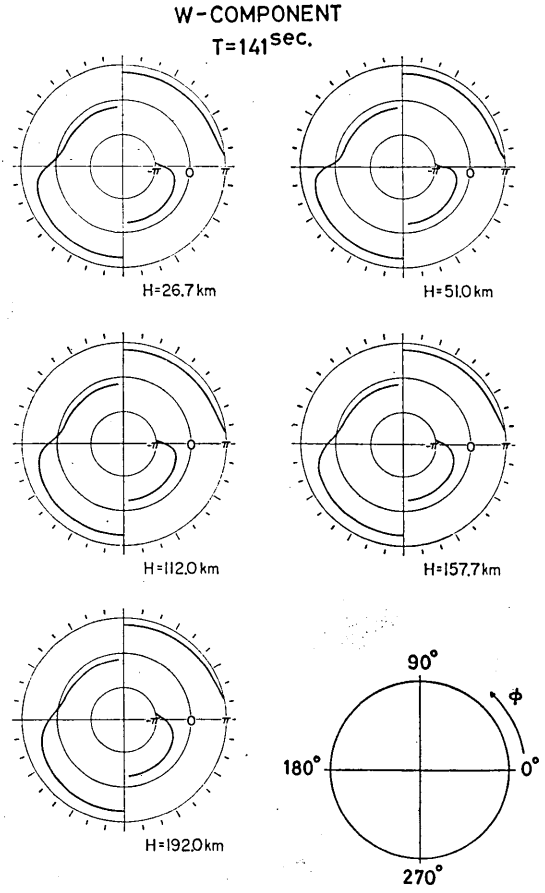

Fig. 12. Azimuthal component of Love wave

Fig. 11~12. Azimuthal variation of the theoretical spatial phase of surface waves generated by normal dip-slip point sources with various focal depths in the Gutenberg-Bullen A′ spherical earth. The dip angle of the fault is fixed as 60°. T and H denote period and focal depth, respectively.

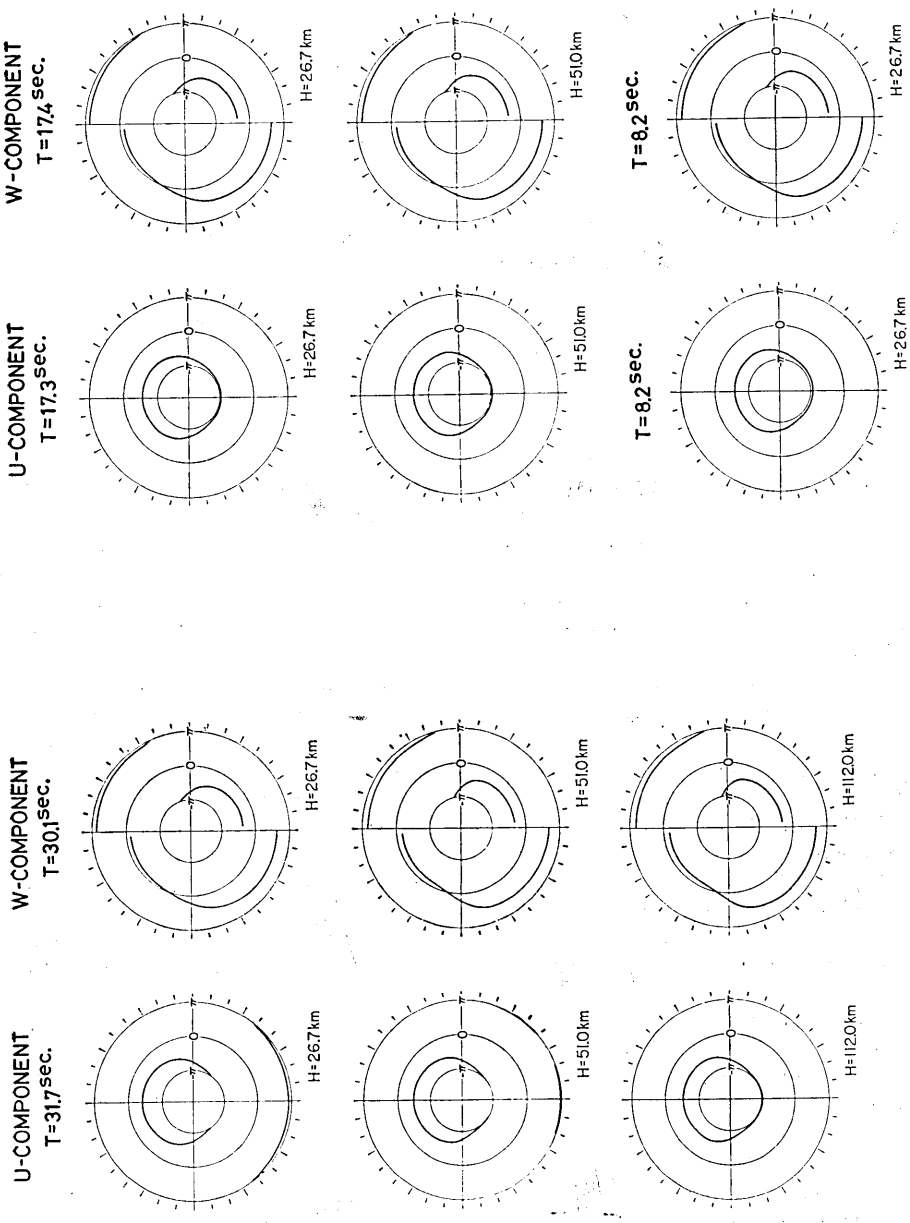

Fig. 13~14. Azimuthal variation of the theoretical spatial phase of radial and azimuthal components. The earth model, the source geometry and the meaning of the notations T and H are the same as in Figures 11~12.

and for the strike-slip case

$$u(r, \theta, \varphi, t) = -u(r, \theta, \pi-\varphi, t), \quad v(r, \theta, \varphi, t) = -v(r, \theta, \pi-\varphi, t), \quad w(r, \theta, \varphi, t) = w(r, \theta, \pi-\varphi, t). \tag{3·7·2}$$

Since only the dip-slip source is considered in the present case, the radial and colatitudinal displacements are symmetrical about the axis of dip direction ($\varphi = 90° \sim 270°$), and the azimuthal component is anti-symmetrical about this axis.

Acknowledgement

The authors wish to express their sincere thanks to Misses K. Ueda, M. Ishida and E. Kawano who assisted them in preparing figures.

References

AKI, K., 1960, Interpretation of source functions of Circum-Pacific earthquakes obtained from long-period Rayleigh waves, *J. Geophys. Res.*, **65**, 2405-2417.

BEN-MENAHEM, A., 1961, Radiation of seismic surface waves from finite moving sources, *Bull. Seism. Soc. Amer.*, **51**, 401-435.

BEN-MENAHEM, A. and M. N. TOKSÖZ, 1963, Source mechanism from spectrums of long-period surface waves, 2. The Kamchatka earthquake of November 4, 1952, *J. Geophys. Res.*, **68**, 5207-5222.

BEN-MENAHEM, A. and D. G. HARKRIDER, 1964, Radiation patterns of seismic surface waves from buried dipolar point sources in a flat stratified earth, *J. Geophys. Res.*, **69**, 2605-2620.

BRUNE, J. N., J. E. NAFE and J. E. OLIVER, 1960, A simplified method for the analysis and synthesis of dispersed wave trains, *J. Geophys. Res.*, **65**, 287-304.

BRUNE, J. N., J. E. NAFE and L. E. ALSOP, 1961, The polar phase shift of surface waves on a sphere, *Bull. Seism. Soc. Amer.*, **51**, 247-257.

BRUNE, J. N., 1961, Radiation pattern of Rayleigh waves from the Southeast Alaska earthquake of July 10, 1958, *Publ. Dominion. Observatory.*, **24**, 373-383.

HASKELL, N. A., 1963, Radiation pattern of Rayleigh waves from a fault of arbitrary dip and direction of motion in a homogeneous medium, *Bull. Seism. Soc. Amer.*, **53**, 619-642.

HASKELL, N. A., 1964, Radiation pattern of surface waves from point sources in a multi-layered medium, *Bull. Seism. Soc. Amer.*, **54**, 377-393.

SATÔ, Y., 1955, 1955, Analysis of dispersed surface waves by means of Fourier transform, I, II and III, *Bull. Earthq. Res. Inst.*, **33**, 33-48, **34**, 9-18, 131-138.

SATÔ, Y., 1958, Attenuation, dispersion, and the wave guide of the G wave, *Bull. Seism. Soc. Amer.*, **48**, 231-251.

SATÔ, Y. and T. USAMI, 1963, Phase angle of waves propagating on a spherical surface with special reference to the polar phase shift and the initial phase, *Bull. Earthq. Res. Inst.*, **41**, 459-466.

TOKSÖZ, M. N. and D. L. ANDERSON, 1966, Phase velocities of long-period surface waves and structure of the upper mantle, *J. Geophys. Res.*, **71**, 1649-1658.

USAMI, T., Y. SATÔ and M. LANDISMAN, 1966, Preliminary study of the propagation of

spheroidal disturbance on the surface of a heterogeneous spherical earth, *Geophys. J.*, **11**, 243-251.

USAMI, T., Y. SATÔ, M. LANDISMAN and T. ODAKA, 1968, Theoretical seismograms of spheroidal type on the surface of a gravitating elastic sphere. III. Case of a homogeneous mantle with a liquid core, *Bull. Earthq. Res. Inst.*, **46**, 791-819.

USAMI, T., T. ODAKA and Y. SATÔ, 1970, Theoretical seismograms and earthquake mechanism, I. Basic principles, II. Effect of time functions on surface waves, *Bull. Earthq. Res. Inst.*, **48**, 533-579.

---

36. 理論地震記象と震源模型

(III) 表面波の初期位相とその方位角方向での変化について

地震研究所 小高俊一
宇佐美龍夫

(I) で述べた方法に基づいてグーテンベルグ・ブレン-A′ 地球モデル中に，dip-slip 型点震源 (dip angle 60°，深さ 5.35 km) を仮定した場合の変位についての理論地震記象を，赤道上の方位角 0° (30°) 330° の各点を含む合計 17 点で計算した．震源での時間関数はランプ型，たち上がり時間約 45 秒を仮定した．自由振動の基準モードのみを採用したので理論地震記象は主に表面波，特に半径方向変位はレーリー波の鉛直成分を，方位角方向変位はラブ波の方位角成分を表わしている．これらの理論地震記象からここで仮定した震源模型についての，振巾と位相の方位角分布の様子が知られる．振巾のそれはレーリー波では二象限型，ラブ波では四象限型に近い型をそれぞれ示すが，位相角は必らずしもそれらの様子とは一致しない．

今回は特に位相角の方位角依存性について調べた．このために先の理論地震記象から，フーリエ解析の方法によって震源における位相角，すなわち初期位相を求めた．これから時間関数の位相角を除いたもの，すなわち震源の空間的性質と地球モデルとによる初期位相 (これを空間的位相角と名づける) を計算した．さらにこの空間的位相角が，自由振動の励起関数から理論的に求められるものと完全に一致することを数値実験的に確かめた．この空間的位相角は，地球モデル，発震機構，震源の深さに依るものであるため，それのパラメターが推定されれば量的に求められるものである．これを用いて実際の地震記象の解析から，震源での時間関数の位相角についての情報を得ることは理論上可能である．

震源の深さがさらに深い場合についても同様の計算を実行した，
